Improving the Frequency Response of DERs Through Voltage Feedback

Georgios Tzounas, *IEEE Student Member*, Federico Milano, *IEEE Fellow*

***Abstract*— This paper studies the ability of Distributed Energy Resources (DERs) to improve, through a proper voltage feedback signal, their primary frequency response by mitigating the part of the injected active power that does not contribute to the frequency regulation. The feedback signal modifies the reference of the DER voltage regulation loop and requires measuring the voltage magnitude at the buses to which the DER is connected. A simplified DER model, as well as a dynamic model of an ESS (Energy Storage System) are employed to test the examined technique through time domain simulations based on the WSCC 9-bus system.**

***Index Terms*— Frequency control, modified voltage control reference, Distributed Energy Resources (DERs), Energy Storage Systems (ESSs).**

I. Introduction

A. Motivation

The frequency regulation capability of modern power systems is challenged by the replacement of synchronous machines from Distributed Energy Resources (DERs). The ability of DERs to regulate the frequency is limited, mainly for two reasons: (i) they are typically designed to operate either under maximum power point tracking control or with a relatively small power reserve; and (ii) a significant part of the power coming from DERs is stochastic – e.g. wind and solar photovoltaic generation – and hence a certain amount of reserve is difficult to be guaranteed [1], [2]. Therefore, there is the need for novel techniques that improve the frequency response of DERs by making efficient use of the available limited power reserve.

B. Literature Review

DERs include a variety of small-size electric energy generation and storage devices connected to a medium or low voltage level, such as solar photovoltaic units, wind turbines, and battery storage [3]. Due to the fact that such devices are connected to the grid through power electronic converters, their increasing penetration in power systems leads to a reduction of rotational inertia which severely impacts the frequency response of the power system [4]. In order to maintain the overall system stability, primary frequency regulation by DERs is considered a necessary service to be provided following a disturbance.

Georgios Tzounas and Federico Milano are with the School of Electrical and Electronic Engineering, University College Dublin, Ireland (e-mails: georgios.tzounas@ucdconnect.ie and federico.milano@ucd.ie).

This material is based upon works funded by European Union's Horizon 2020 research and innovation programme, under grant agreement No. 883710. The authors are also supported by the Science Foundation Ireland, under Investigator Programme Grant No. SFI/15/IA/3074.

An advantage of power electronic converters is that they can be effectively designed to provide fast regulation. This feature, in particular the provision of fast frequency regulation provided by DERs has been duly discussed in the literature [5], [6]. The capabilities for frequency support have been explored for different DER technologies, including wind turbines, Energy Storage Systems (ESSs), photovoltaic generation, controllable loads, and the concept of virtual power plants [7]–[12]. Moreover, a comparison of different control strategies to generate the signal used as input to DER frequency regulation loops was provided in [13].

Recently, the second author of this paper presented a practical criterion to evaluate, through local measurements of frequency variations, the frequency control provided by a grid-connected device in transient conditions [14]. The proposed criterion, which is based on the concept of the frequency divider formula [15], is derived by utilizing the "regulating" active power, i.e. the quota of injected active power that depends on the frequency variations at the system buses. Applications of this criterion to non-synchronous devices, including wind turbines and ESSs, are provided in [16]. The theoretical foundations of [14] and [15] serve as inspiration for the novel control approach of DERs proposed in this paper.

C. Contribution

This paper presents a technique to improve the effectiveness of the primary frequency control provided by DERs through synthesizing a proper voltage-based feedback signal. This feedback signal is utilized to modify the reference of the DER voltage control loop. The paper shows that this feedback on the voltage control is able to improve the efficiency of the frequency control loop. In turn, given a certain power reserve, the proposed control strategy allows improving the frequency response of the system or, equivalently, given a target frequency response, the proposed strategy allows achieving it with less power reserve.

D. Organization

The remainder of the paper is organized as follows. Section II briefly describes the structure of the frequency and voltage control for the simplified DER and ESS models that are employed to test the proposed technique. Section III provides an analytical derivation of the voltage-based signal feedback used to modify the reference of the voltage control loop. Section IV discusses a case study based on a modified version of the well-known WSCC 9-bus system. Finally, conclusions and future work directions are discussed in Section V.

II. Modeling

This section briefly describes the basic control structure of a simplified DER and ESS models. These models are then utilized in the case study presented in Section IV.

The block diagram of the DER model is depicted in Fig. 1. It consists of an inner control loop, that regulates the components $\imath_{\rm d}$, $\imath_{\rm q}$ of the current in the dq reference frame, and two outer loops for frequency and voltage control, respectively. The frequency control loop filters the frequency error $\omega^{\rm ref} - \omega$ and implements a droop control with droop constant R. The frequency control output is then added to the DER's active power reference. On the other hand, the voltage control loop receives the error $v^{\rm ref} - v_{{\rm B},h}$ and implements a Proportional-Integral (PI) control. The output of the voltage control loop is added to the DER's reactive power reference.

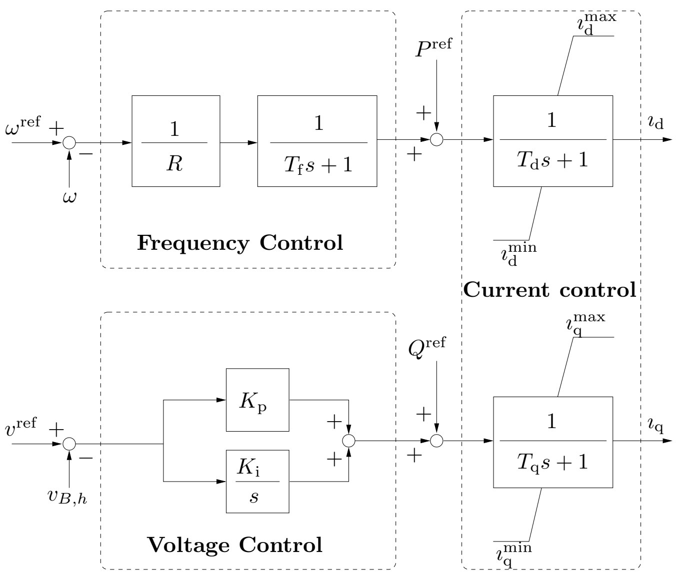

Fig. 1: Simplified DER control diagram.

The control structure of the ESS model is shown in Fig. 2. The frequency control loop filters the frequency error and implements a lead-lag regulator with droop constant $R = H_{\rm P}/(K_{{\rm i},P} + K_{{\rm p},P} H_P)$, the output of which is fed to the ESS active power dynamics. The voltage control loop filters the voltage error and implements a lead-lag control, the output of which is input to the ESS reactive power dynamics.

In standard voltage control schemes, such as those shown in Figs. 1 and 2, the voltage reference is constant, at least for a given period, hence:

$$v^{\rm ref}(t) = v_o^{\rm ref} = v_{{\rm B},h,o} \, , \tag{1}$$

where $v_o^{\rm ref}$ is the desired reference voltage and $v_{{\rm B},h,o}$ denotes the value, in steady-state, of the voltage magnitude at bus h where the DER is connected. In this paper, we examine the effectiveness of modifying (1) by using a feedback signal that aims to mitigate the part of the injected active power that does not contribute to frequency regulation. The modified voltage control reference is analytically derived in the next section.

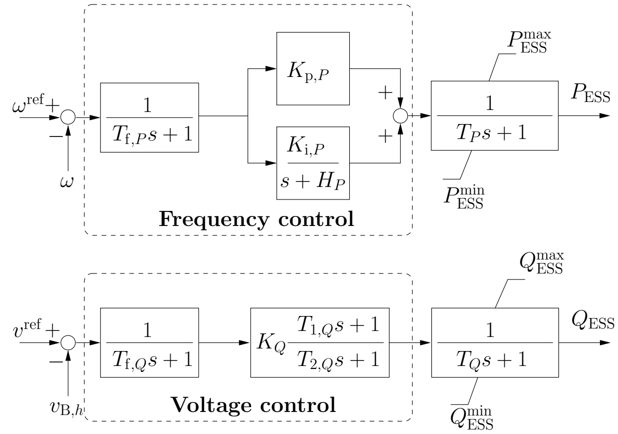

Fig. 2: Simplified ESS control diagram of and model.

III. Proposed Control with Modified Voltage Control Reference

This section describes the proposed control with modified voltage control reference to improve the frequency response provided by DERs. To this aim, we start from the well-known power flow equations. The complex power $\bar{\boldsymbol{s}}_{\rm B}$ injected at the buses of a power network can be expressed as follows:

$$\bar{\boldsymbol{s}}_{\rm B}(t) = \boldsymbol{p}_{\rm B}(t) + j\boldsymbol{q}_{\rm B}(t) = \bar{\boldsymbol{v}}_{\rm B}(t) \circ \left(\bar{\mathbf{Y}}\, \bar{\boldsymbol{v}}_{\rm B}(t)\right) \, , \tag{2}$$

where $\boldsymbol{p}_{\rm B}, \boldsymbol{q}_{\rm B} \in \mathbb{C}^{n\times 1}$ are the vectors of bus active and reactive power injections, respectively, with n being the number of network buses; $\bar{\mathbf{Y}} \in \mathbb{C}^{n\times n}$ is the network admittance matrix; $\bar{\boldsymbol{v}}_{\rm B} \in \mathbb{C}^{n\times 1}$ is the vector of bus voltages; and $\circ$ denotes the Hadamard product, i.e., the element-wise multiplication.

From (2), the h-th element of $\boldsymbol{p}_{\rm B}$ can be written as follows:

$$\begin{aligned} p_{{\rm B},h}(t) &= v_{{\rm B},h}(t) \sum_{k\in\mathbb{B}} v_{{\rm B},k}(t)\, G^{hk}\, \cos\theta_{{\rm B},hk}(t) \\ &+ v_{{\rm B},h}(t) \sum_{k\in\mathbb{B}} v_{{\rm B},k}(t)\, B^{hk}\, \sin\theta_{{\rm B},hk}(t) \, , \end{aligned} \tag{3}$$

where $\mathbb{B}$ is the set of network buses; G^{hk} and B^{hk} are the real and imaginary parts of the (h,k) element of matrix $\bar{\mathbf{Y}}$, i.e. $\bar{Y}^{hk} = G^{hk} + jB^{hk}$; $v_{{\rm B},h}$ and $v_{{\rm B},k}$ are the voltage magnitudes at buses h and k, respectively, at time t; and $\theta_{{\rm B},hk} = \theta_{{\rm B},h} - \theta_{{\rm B},k}$, where $\theta_{{\rm B},h}$ and $\theta_{{\rm B},k}$ are the voltage phase angles at buses h and k, respectively.

Differentiating (3) allows deriving the deviation of the active power injection at bus h as a sum of two components [14]:

$$dp_{{\rm B},h} = dp'_{{\rm B},h} + dp''_{{\rm B},h} \, , \tag{4}$$

where

$$dp'_{{\rm B},h} = \sum_{k\in\mathbb{B}} \frac{\partial p_{{\rm B},h}}{\partial \theta_{{\rm B},k}} d\theta_{{\rm B},k} \, , \tag{5}$$

$$dp''_{{\rm B},h} = \sum_{k\in\mathbb{B}} \frac{\partial p_{{\rm B},h}}{\partial v_{{\rm B},k}} \, dv_{{\rm B},k} \, . \tag{6}$$

The term $dp'_{{\rm B},h}$ is the component of the active power that can effectively modify or impact the frequency in the grid. This observation is the key of the control proposed in this paper. To better illustrate this point, one can consider expression (5) with respect to time and substitute $\frac{d\theta_{{\rm B},k}}{dt} = \Omega_b\, \omega_{{\rm B},k}$, where $\omega_{{\rm B},k}$ is the frequency at bus k and Ω_b is the reference synchronous speed in rad/s. On the other hand, the term $dp''_{\mathrm{B},h}$ mainly depends on the variations of the bus voltage magnitudes and, thus, has a negligible impact on the frequency response of the system.

A device that regulates the frequency imposes $dp_{\mathrm{B},h}$ at its point of connection. Thus, the idea proposed in this paper is to design a control that has the objective to reduce – ideally, to nullify – the term $dp''_{\mathrm{B},h}$. Since this term does not contribute to the frequency response of the system, the effect is to make $dp_{\mathrm{B},h} \approx dp'_{\mathrm{B},h}$ and, hence, optimize the effectiveness of the frequency control. The proposed control, in turn, is designed to impose the following constraint:

$$dp''_{\mathrm{B},h} = 0 \,. \tag{7}$$

Using (3), and assuming for simplicity a lossless transmission system, i.e. $G^{hk} = 0$, and defining $\tilde{B}^{hk} = B^{hk} \sin\theta_{\mathrm{B},hk}$, we can rewrite (6) as follows:

$$dp''_{\mathrm{B},h} = \sum_{k\in\mathbb{B}} \tilde{B}^{hk}(t)\, d[v_{\mathrm{B},h}(t)\, v_{\mathrm{B},k}(t)] \,, \tag{8}$$

or, equivalently,

$$dp''_{\mathrm{B},h} = \sum_{k\in\mathbb{B}} \tilde{B}^{hk}(t) \left(v_{\mathrm{B},k}\, dv_{\mathrm{B},h} + v_{\mathrm{B},h}\, dv_{\mathrm{B},k}\right) . \tag{9}$$

From (9), a sufficient condition so that (7) is satisfied reads as follows:

$$\sum_{k\in\mathbb{B}} \left(v_{\mathrm{B},k}(t)\, dv_{\mathrm{B},h} + v_{\mathrm{B},h}(t)\, dv_{\mathrm{B},k}\right) = 0 \,. \tag{10}$$

The last equation is equivalent to:

$$v_{\mathrm{B},h}(t) \sum_{k\in\mathbb{B}} v_{\mathrm{B},k}(t) = c_o \,, \tag{11}$$

where c_o is a constant, which, following from the system initialization, takes the value:

$$c_o = v_{\mathrm{B},h,o}(t) \sum_{k\in\mathbb{B}} v_{\mathrm{B},k,o}(t) \,. \tag{12}$$

From the above analysis, we get that the modified voltage control reference that can be utilized to achieve the control objective (7) is:

$$v^{\mathrm{ref}}(t) = \frac{c_o}{\sum_{k\in\mathbb{B}} v_{\mathrm{B},k}(t)} \,. \tag{13}$$

Note that (13) is valid also for lossy transmission systems, i.e. $G^{hk} \neq 0$,and is, thus, a general condition.

The implementation of (13) requires measuring the voltage magnitudes at the buses to which the DER is connected which in turn depends on the topology of the system. Figure 3a shows a DER connected to the grid in antenna. In this case, only one remote measurement is needed, namely $v_{\mathrm{B},2}$. If the DER is connected to the grid through multiple buses, more measurements are required. For example, in the topology shown in Fig. 3b, one has to measure $v_{\mathrm{B},2}$ and $v_{\mathrm{B},3}$.

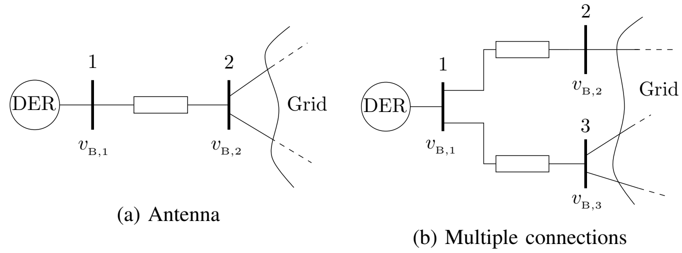

Fig. 3: Examples of DER connectivity to the grid.

IV. Case Study

This section presents simulation results based on a modified version of the well-known WSCC 9-bus test system [17]. The modified test system is shown in Fig. 4. The network comprises 6 transmission lines and 3 medium voltage/high voltage transformers; the Synchronous Machine (SM) connected to bus 1 is modeled with a fourth order, two-axis model, and is equipped with a turbine governor and automatic voltage regulation; during transients, loads are modeled as constant admittances.

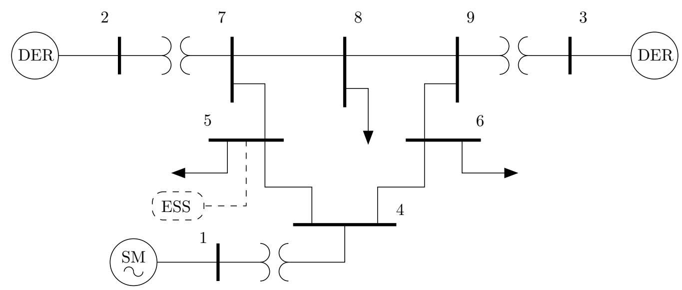

Fig. 4: Modified WSCC 9-bus system.

The modifications with respect to the original system are as follows. The generators at buses 2 and 3 have been replaced by DERs represented according to the model described in Section II. The parameters used for the DER current, frequency, and voltage controllers are given in Table I. Then, the mechanical starting time of the SM connected to bus 1 is decreased to 23 s. With the above changes, the inertia of the system has been reduced by 65% compared to the data of the original system. Finally, in Section IV-B an ESS is connected to bus 5. The parameters used for the ESS controls are given in Table II. All simulation results in this section are obtained using the power system analysis software tool Dome [18].

TABLE I: Parameters of DER control

Controller	Parameters
Current	$T_{\mathrm{d}} = 0.6$ s, $T_{\mathrm{q}} = 0.6$ s
Frequency	$R = 0.06$, $T_{\mathrm{f}} = 1.2$ s
Voltage	$K_{\mathrm{i}} = 5$, $K_{\mathrm{p}} = 10$

TABLE II: Parameters of ESS control

Controller	Parameters
Current	$T_P = 0.1$ s, $T_Q = 0.1$ s,
Frequency	$T_{\mathrm{f},P} = 0.2$ s, $K_{\mathrm{i},P} = 5$, $K_{\mathrm{p},P} = 10$, $H_P = 0.5$
Voltage	$T_{\mathrm{f},Q} = 0.2$ s, $K_Q = 3$, $T_{1,Q} = 1$ s, $T_{2,Q} = 1.8$ s

A. DERs Connected to Buses 2 and 3

We test the impact of voltage reference (13) on the frequency regulation provided by the DERs connected to buses 2 and 3 of the modified WSCC 9-bus system. In this scenario, no ESS is included in the system. To this aim, we compare the following scenarios for the DER control:

1) CPC (Constant Power Control), i.e. without the frequency and voltage control loops;
2) FC, i.e. with the frequency loop connected and the voltage control disconnected;
3) FC+VC, i.e. with both frequency and voltage control connected and the voltage control reference given by (1);
4) FC+MRVC, i.e. with both frequency and voltage control connected and with the modified voltage control reference given by (13).

The scenarios that include frequency regulation, i.e. (ii), (iii) and (iv), consider as frequency control input signal the frequency of the center of inertia, which, since there is only one SM left in the system, coincides with the rotor speed of the SM connected to bus 1 ($\omega_{\mathrm{r},1}$). Moreover, for the FC+MRVC, the DERs at buses 2 and 3 are connected to the transmission system in antenna and thus require the voltage magnitudes at buses 7 ($v_{\mathrm{B},7}$) and 9 ($v_{\mathrm{B},9}$), respectively, to implement reference (13).

We consider the transient that follows the tripping, at $t = 1$ s, of the line that connects buses 4 and 6. Simulation results are presented in Figs. 5-7. In particular, Fig. 5 shows the trajectory of the rotor speed of the SM (in Hz) following the disturbance. The system dynamic behavior for the CPC and FC is not acceptable, while for the examined disturbance, inclusion of the voltage control loop significantly improves the frequency response. The proposed FC+MRVC provides a further significant improvement in the frequency regulation (> 0.1 Hz) with respect to the FC. A comparison of the voltage references of the FC+MRVC and FC+VC for the DER connected to bus 2 is shown in Fig. 6. It is important to note that the improvement provided by the FC+MRVC comes without jeopardizing the voltage response of the system. This is shown in Fig. 7. Overall, in the case of a line trip, the FC+MRVC provides an important improvement in the frequency regulation of the system. We have applied trips to other lines of the network and obtained similar results and same conclusions.

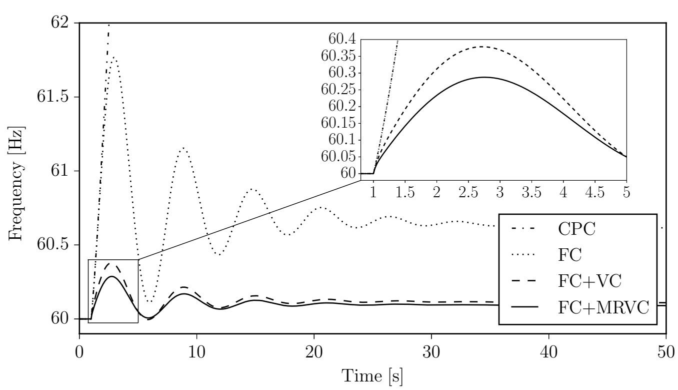

Fig. 5: Frequency response following the outage of line 4-6.

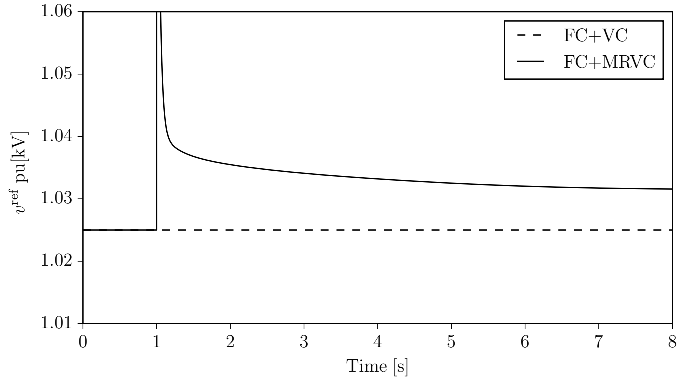

Fig. 6: DER connected to bus 2: voltage reference following the outage of line 4-6.

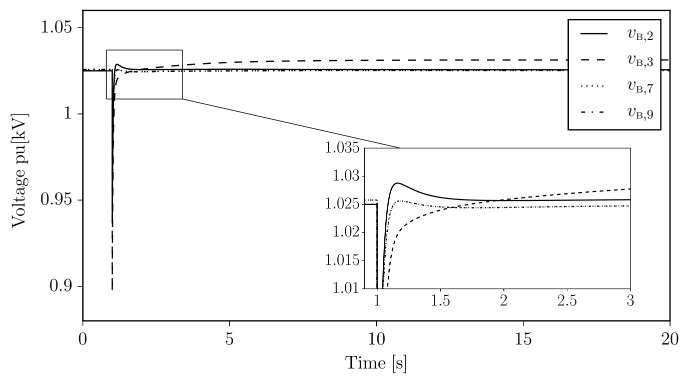

Fig. 7: FC+MRVC: voltage response following the outage of line 4-6.

B. ESS Connected to Bus 5

In this scenario, an ESS is connected to bus 5 of the modified WSCC 9-bus system. The objective is to assessing the impact of the FC+MRVC on the primary frequency response provided by the ESS. With this aim, in this scenario, the DERs connected to buses 2 and 3 do not provide frequency and voltage control (see CPC in Section IV-A).

The test system is simulated considering a three-phase fault at bus 6. The fault occurs at $t = 1$ s and is cleared after 80 ms by tripping the line that connects buses 6 and 9. Two control modes are compared for the ESS control: FC+VC and FC+MRVC. The voltage reference (13) of the FC+MRVC is implemented with the measurements of the voltage magnitudes at buses 4 and 7. The frequency response of the system is shown in Fig. 8. The FC+MRVC provides a significant improvement in the frequency regulation of the system, while this is achieved in an economic way, since a lower variation of the stored energy is required (see Fig. 9).

We have thoroughly tested the dynamic behavior of the modified 9-bus system with inclusion of the FC+MRVC for a variety of different contingencies. There exist scenarios for which the difference between the FC+MRVC and FC+VC is smaller than the cases shown in Figs. 5 and 8. In Fig. 10, we consider a 15% sudden increase of the susceptance and conductance of all system loads occurring at $t = 1$ s. In this case, FC+VC and FC+MRVC show substantially the same dynamic behavior. In general, we can conclude that the proposed FC+MRVC, in the cases where it is not beneficial, at least does not worsen the dynamic response of the system.

V. Conclusions

This paper presents a new technique based on a voltage feedback that improves the effectiveness of the primary frequency control provided by DERs. The proposed technique requires remote bus voltage measurements and consists in modifying the reference of the DER voltage control loop. Simulation results show that the proposed control provides a significant improvement of the frequency regulation for a class of disturbances, e.g., short-circuits and line outages.

We will dedicate future work to improve the effectiveness of the proposed technique as well as to test it in the presence of communication phenomena, such as measurement delays and noise.

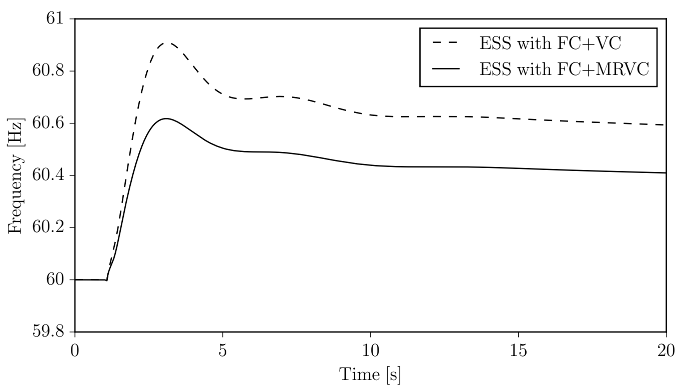

Fig. 8: Frequency response following a three-phase fault.

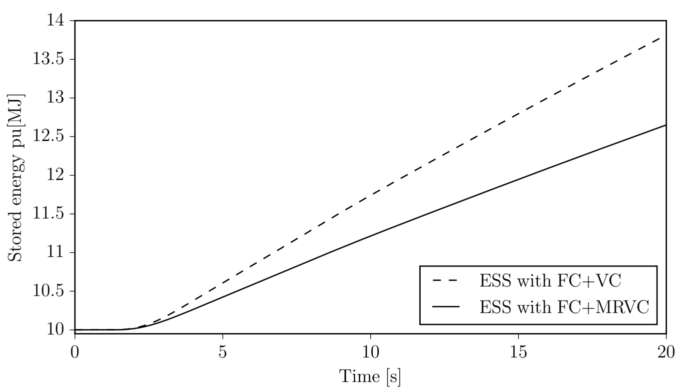

Fig. 9: ESS stored energy following a three-phase fault.

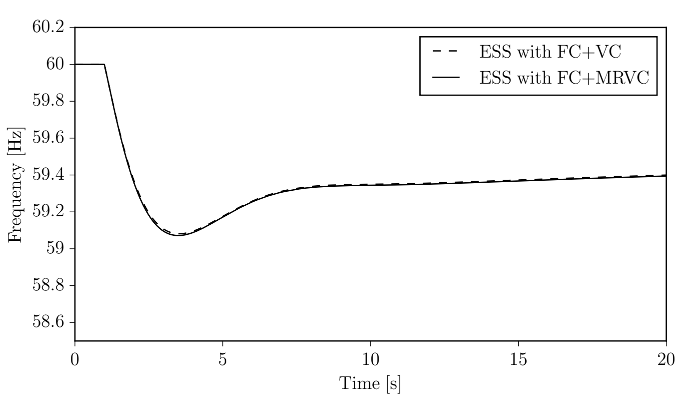

Fig. 10: Frequency response following a load increase.

References

[1] J. M. Mauricio, A. Marano, A. Gómez-Expósito, and J. L. Martínez Ramos, "Frequency regulation contribution through variable-speed wind energy conversion systems," *IEEE Transactions on Power Systems*, vol. 24, no. 1, pp. 173–180, 2009.

[2] F. Milano, F. Dörfler, G. Hug, D. J. Hill, and G. Verbič, "Foundations and challenges of low-inertia systems (invited paper)," in *Proceedings of the Power Systems Computation Conference*, 2018, pp. 1–25.

[3] M. F. Akorede, H. Hizam, and E. Pouresmaeil, "Distributed energy resources and benefits to the environment," *Renewable and Sustainable Energy Reviews*, vol. 14, no. 2, pp. 724 – 734, 2010.

[4] A. Ulbig, T. S. Borsche, and G. Andersson, "Impact of low rotational inertia on power system stability and operation," *IFAC Proceedings Volumes*, vol. 47, no. 3, pp. 7290 – 7297, 2014, 19th IFAC World Congress.

[5] M. F. M. Arani and E. F. El-Saadany, "Implementing virtual inertia in DFIG-based wind power generation," *IEEE Transactions on Power Systems*, vol. 28, no. 2, pp. 1373–1384, 2013.

[6] IEEE, "Contribution to bulk system control and stability by distributed energy resources connected at distribution network," *Technical Report PES-TR22*, Jan. 2017.

[7] G. Ramtharan, J. B. Ekanayake, and N. Jenkins, "Frequency support from doubly fed induction generator wind turbines," *IET Renewable Power Generation*, vol. 1, no. 1, pp. 3–9, 2007.

[8] Y. Liu, H. Xin, Z. Wang, and D. Gan, "Control of virtual power plant in microgrids: a coordinated approach based on photovoltaic systems and controllable loads," *IET Generation, Transmission & Distribution*, vol. 9, no. 10, pp. 921–928, 2015.

[9] J. Zhao, X. Lyu, Y. Fu, X. Hu, and F. Li, "Coordinated microgrid frequency regulation based on DFIG variable coefficient using virtual inertia and primary frequency control," *IEEE Transactions on Energy Conversion*, vol. 31, no. 3, pp. 833–845, 2016.

[10] M. Ramírez, R. Castellanos, G. Calderón, and O. Malik, "Placement and sizing of battery energy storage for primary frequency control in an isolated section of the Mexican power system," *Electric Power System Research*, vol. 160, pp. 142 – 150, 2018.

[11] D. Koraki and K. Strunz, "Wind and solar power integration in electricity markets and distribution networks through service-centric virtual power plants," *IEEE Transactions on Power Systems*, vol. 33, no. 1, pp. 473–485, 2018.

[12] A. Fathi, Q. Shafiee, and H. Bevrani, "Robust frequency control of microgrids using an extended virtual synchronous generator," *IEEE Transactions on Power Systems*, vol. 33, no. 6, pp. 6289–6297, 2018.

[13] Á. Ortega and F. Milano, "Frequency control of distributed energy resources in distribution networks," *IFAC-PapersOnLine*, vol. 51, no. 28, pp. 37 – 42, 2018, IFAC Symposium on Control of Power and Energy Systems.

[14] F. Milano and Á. Ortega, "A method for evaluating frequency regulation in an electrical grid Part I: Theory," *IEEE Transactions on Power Systems*, 2020, pre-print available on ieeexplore.ieee.org.

[15] ——, "Frequency divider," *IEEE Transactions on Power Systems*, vol. 32, no. 2, pp. 1493–1501, Mar. 2017.

[16] Á. Ortega and F. Milano, "A method for evaluating frequency regulation in an electrical grid Part II: Applications to non-synchronous devices," *IEEE Transactions on Power Systems*, 2020, pre-print available on ieeexplore.ieee.org.

[17] P. Sauer and M. Pai, *Power System Dynamics and Stability*. Prentice Hall, 1998.

[18] F. Milano, "A Python-based software tool for power system analysis," in *Proceedings of the IEEE PES General Meeting*, Jul. 2013.